PERFORMANCE BOUNDS FOR JOINT ESTIMATION OF IONOSPHERIC AND TARGET PARAMETERS IN MIMO-OTH RADAR

Mao Li, Qian He, Zishu He, and Rick S.Blum*[†]

EE Department, Univ. of Electron. Sci. and Tech. of China, Chengdu, Sichuan 611731 China
[†]ECE Department, Lehigh University, Bethlehem, PA 18015 USA

ABSTRACT

Ionospheric information is required when estimating target parameters in skywave over-the-horizon (OTH) radar. Unlike the traditional OTH radar which uses only the measurements of ionospheric parameters obtained from an ionosonde to estimate the target parameters, the multiple-input multiple-output skywave OTH (MIMO-OTH) radar studied in this paper estimates the ionospheric and target parameters jointly by exploiting the data received by both the ionosonde and the radar receivers. Two scenarios where the prior distribution of the ionospheric parameters is either known or unknown are considered. For the case when ionospheric parameter prior distribution is unknown, the joint maximum likelihood (JML) estimator is investigated and the Cramér-Rao bound (CRB) is derived. For the case when the ionospheric parameter prior distribution is known, the hybrid maximum likelihood and the maximum a posteriori (ML/MAP) estimator is studied and the hybrid Cramér-Rao bound (HCRB) is developed.

***Index Terms*—** MIMO-OTH radar, joint estimation, ionospheric parameters, target parameters.

1. INTRODUCTION

Sky wave over-the-horizon (OTH) radar operates in 3-30MHz, which can provide over the horizon detection of targets in large surveillance areas [1]. In recent years, multiple-input multiple-output (MIMO) radar techniques [2–7] have been applied to the OTH radar. In [8], a novel technique is developed for altitude estimation of a maneuvering target using a MIMO-OTH radar. The clutter mitigation performance of a MIMO-OTH radar is analyzed in [9].

In OTH radar, the non-stationary ionosphere helps determine the propagation paths for both transmitted and backscattered signals. Further, the performance of an OTH radar greatly depends on the accuracy with which the system knows the ionospheric parameters. The ionospheric parameters are usually estimated using an ionosonde [10]. Traditional OTH radar takes the estimated ionospheric parameters as known quantities and uses them for target parameter estimation [11–15]. Estimation errors of the ionospheric parameters introduced by the ionosonde can dramatically degrade the target parameter estimation performance of the OTH radar system. Actually, since both the transmitted and backscattered signals of OTH radar traverse through the ionosphere, the received signals should carry abundant information about the state of the ionosphere. The use of this information can improve the accuracy of target estimation.

In this paper, MIMO-OTH radar is employed to estimate the ionospheric and target parameters jointly, using the measurements from both the ionosonde and the radar system. The optimum estimators are presented for the cases where the ionospheric parameters have either a known and unknown prior distribution and the corresponding performance bounds are derived.

2. SIGNAL MODEL

Consider a MIMO-OTH radar with M transmitters and N receivers in a two-dimensional Cartesian space. The complex envelop of the signal transmitted by the mth transmitter is $\sqrt{E_m}s_m(t)$, where E_m is the transmitted energy and $s_m(t), m = 1, \ldots, M$, are a set of unit energy waveforms which are approximately orthogonal for any time delay τ and Doppler shift f_d of interest [7], such that $\int_{T_r} s_m(t)s^*_{m'}(t-\tau)e^{j2\pi f_d t}dt$ equals 1 for $m = m'$ and 0 for $m \neq m'$ and integration is taken over a pulse repetition interval T_r. For simplicity the flat-earth model is adopted. The positions of the mth transmitter and the nth receiver are denoted by $(x^T_m, 0)$ and $(x^R_n, 0)$, respectively[1]. Suppose a target is moving with constant velocity v along the x-axis and its initial position is $(x, 0)$, where x and v are assumed to be deterministic but unknown. We use a parabolic layer model [10] to describe the characteristics of the ionosphere, in which the electron density at height[2] y is given by

*Correspondence: qianhe@uestc.edu.cn.

This work was supported by the National Nature Science Foundation of China under Grants 61102142 and 61032010, the International Science and Technology Cooperation and Exchange Research Program of Sichuan Province under Grant 2013HH0006, the Fundamental Research Funds for the Central Universities under Grant ZYGX2013J015, and by the National Science Foundation under Grant CCF-0829958.

[1]For simplicity, we assume the antennas and target are on a line but generalization is straightforward.

[2]Throughout this paper, "height" means *height above the ground*.

978-1-4799-2893-4/14/$31.00 ©2014 IEEE

$$d(y) = \begin{cases} \frac{f_o^2}{80.6}[1-(\frac{y-y_o}{a})^2] & |y-y_o| < a \\ 0 & otherwise \end{cases} \quad (1)$$

where y_o denotes the height of the ionosphere with maximum electron density, f_o denotes the critical frequency, $a = y_o - y_b$ is the semi-layer thickness, and y_b is the base height of the ionospheric layer. The ionospheric parameters y_o, y_b, and f_o are assumed to be unknown. Denote the vector composed of all the unknown parameters as

$$\boldsymbol{\theta} = [x, v, y_o, y_b, f_o]^T = [\boldsymbol{\phi}^T, \boldsymbol{\psi}^T]^T \quad (2)$$

where $\boldsymbol{\phi} = [x, v]^T$ contains all the unknown target parameters and $\boldsymbol{\psi} = [y_o, y_b, f_o]^T$ contains all the unknown ionospheric parameters. We break up time into intervals of duration T_r and associate the kth interval with the slow time index k. Denote the signal at the output of the matched filter (matched to $s_m(t)$) at the nth receiver due to the transmission of the mth transmitter at slow time k by $r_{mn}(k)$. Collect signals from K consecutive slow times in a column vector[3]

$$\begin{aligned} \boldsymbol{r}_{mn} &= [r_{mn}(1), \cdots, r_{mn}(K)]^T \\ &= \sqrt{E_m}\alpha_{mn}\boldsymbol{T}_{mn}(\boldsymbol{\theta}) + \boldsymbol{w}_{mn} \end{aligned} \quad (3)$$

where α_{mn} is the target reflection coefficient of the mnth path which is assumed to be a zero-mean complex Gaussian random variable with known variance σ_{mn}^2. Assume that the target reflection coefficients for different paths are statistically independent of each other and remain approximately constant over the observation interval. The noise vector $\boldsymbol{w}_{mn} = [w_{mn}(1), \cdots, w_{mn}(K)]^T$ in (3) is assumed to be zero-mean complex Gaussian and $\mathbb{E}(w_{mn}(k)w_{mn}^*(k')) = \sigma^2\delta(k-k')$, where $\delta(k)$ is a unit impulse function. Assume that the noise components $\boldsymbol{w}_{mn}$ for different mn are independent, and that the target reflection coefficients and the noise are mutually independent. The term $\boldsymbol{T}_{mn}(\boldsymbol{\theta})$ in (3) is given by

$$\boldsymbol{T}_{mn}(\boldsymbol{\theta}) = [e^{j2\pi\varphi_{mn}(\boldsymbol{\theta},1)}, \cdots, e^{j2\pi\varphi_{mn}(\boldsymbol{\theta},K)}]^T \quad (4)$$

where $\varphi_{mn}(\boldsymbol{\theta}, k) = -f_m\tau_{mn}(\boldsymbol{\theta}, k)$ and f_m is the carrier frequency of the signal transmitted at transmitter m. The time delay $\tau_{mn}(\boldsymbol{\theta}, k)$ corresponding to the mnth path is given by $\tau_{mn}(\boldsymbol{\theta}, k) = P_m^F(\boldsymbol{\theta}, k)/c + P_n^B(\boldsymbol{\theta}, k)/c$ where c denotes the velocity of light and $P_m^F(\boldsymbol{\theta}, k)$ denotes the group path length [16] between the mth transmitter and the target obtained from the parabolic layer modeled (1) [16], which is

$$P_m^F(\boldsymbol{\theta}, k) = \frac{2y_b}{\sin\beta_m^F(\boldsymbol{\theta}, k)} + ab\ln\frac{1 + b\sin\beta_m^F(\boldsymbol{\theta}, k)}{1 - b\sin\beta_m^F(\boldsymbol{\theta}, k)} \quad (5)$$

with $b = f_m/f_o$ and $\beta_m^F(\boldsymbol{\theta}, k)$ denoting the transmitting elevation angle which, according to the Breit-Tuve theorem [10], should satisfy

$$\frac{2y_b}{\sin\beta_m^F(\boldsymbol{\theta}, k)} + ab\ln\frac{1 + b\sin\beta_m^F(\boldsymbol{\theta}, k)}{1 - b\sin\beta_m^F(\boldsymbol{\theta}, k)} = \frac{x + vkT_r - x_m^T}{\cos\beta_m^F(\boldsymbol{\theta}, k)}. \quad (6)$$

The group path $P_n^B(\boldsymbol{\theta}, k)$ between the nth receiver and the target can be derived in a similar way by replacing $\beta_m^F(\boldsymbol{\theta}, k)$ and x_m^T with $\beta_n^B(\boldsymbol{\theta}, k)$ and x_n^R in (5) and (6), where $\beta_n^B(\boldsymbol{\theta}, k)$ denotes the receiving elevation angle. For later use, we define a $KMN \times 1$ column vector

$$\boldsymbol{r} = [\boldsymbol{r}_{11}^T, \boldsymbol{r}_{12}^T, \cdots, \boldsymbol{r}_{1N}^T, \boldsymbol{r}_{21}^T, \cdots, \boldsymbol{r}_{MN}^T]^T \quad (7)$$

to stack the received signals from all paths.

[3]Note that clutter is not included in the signal model, considering that they can be eliminated in the preprocessing.

3. JOINT ESTIMATION OF IONOSPHERIC AND TARGET PARAMETERS

Different from the conventional OTH radars, where the ionospheric parameters are estimated by the ionosonde independently and then passed to the OTH radar as known quantities for estimating target parameters, this section considers MIMO-OTH radar and estimates the ionospheric and target parameters jointly using the measurements obtained from both the ionosonde and the radar. The joint estimator is first derived for the case where the prior distribution of the ionospheric parameters is either known or unknown.

3.1. Estimation With Unknown Ionospheric Parameter Distribution

For the joint estimators, both the output of the ionosonde and the MIMO-OTH radar received signal vector in (7) are used as our measurements. Denote the ionosonde output by $\hat{\boldsymbol{\psi}}$, an estimate of the ionospheric parameter vector $\boldsymbol{\psi}$, which can be expressed as

$$\hat{\boldsymbol{\psi}} = \boldsymbol{\psi} + \boldsymbol{w}_{\hat{\boldsymbol{\psi}}} \quad (8)$$

where $\boldsymbol{w}_{\hat{\boldsymbol{\psi}}} = \hat{\boldsymbol{\psi}} - \boldsymbol{\psi}$ denotes the ionosonde measurement error, which is assumed to be zero-mean Gaussian distributed with known variance $\boldsymbol{V}$.

When the prior distribution of the ionospheric parameters is unknown, the unknown parameter vector is deterministic unknown. Under the assumption that $\boldsymbol{w}_{mn}$, α_{mn} in (3), and $\boldsymbol{w}_{\hat{\boldsymbol{\psi}}}$ in (8) are independent of each other, the likelihood function can be written as

$$p(\boldsymbol{r}, \hat{\boldsymbol{\psi}}|\boldsymbol{\theta}) = p(\boldsymbol{r}|\hat{\boldsymbol{\psi}}, \boldsymbol{\theta})p(\hat{\boldsymbol{\psi}}|\boldsymbol{\theta}) = p(\boldsymbol{r}|\boldsymbol{\theta})\, p(\hat{\boldsymbol{\psi}}|\boldsymbol{\psi}). \quad (9)$$

where, from (3) and (7),

$$p(\boldsymbol{r}|\boldsymbol{\theta}) = \prod_{m=1}^{M}\prod_{n=1}^{N} p(\boldsymbol{r}_{mn}|\boldsymbol{\theta}) \quad (10)$$

in which

$$p(\boldsymbol{r}_{mn}|\boldsymbol{\theta}) = \frac{1}{\det(\pi\boldsymbol{C}_{mn}(\boldsymbol{\theta}))} e^{-\boldsymbol{r}_{mn}^H\boldsymbol{C}_{mn}^{-1}(\boldsymbol{\theta})\boldsymbol{r}_{mn}},$$

$$\boldsymbol{C}_{mn}(\boldsymbol{\theta}) = \sigma^2\boldsymbol{I} + E_m\sigma_{mn}^2\boldsymbol{T}_{mn}(\boldsymbol{\theta})\boldsymbol{T}_{mn}^H(\boldsymbol{\theta}),$$

$$\boldsymbol{C}_{mn}^{-1}(\boldsymbol{\theta}) = \frac{1}{\sigma^2}\boldsymbol{I} - \frac{E_m\sigma_{mn}^2}{\sigma^2(\sigma^2 + KE_m\sigma_{mn}^2)}\boldsymbol{T}_{mn}(\boldsymbol{\theta})\boldsymbol{T}_{mn}^H(\boldsymbol{\theta}),$$

$$\det(\boldsymbol{C}_{mn}(\boldsymbol{\theta})) = \sigma^{2K}(1 + KE_m\sigma_{mn}^2/\sigma^2),$$

and

$$p(\hat{\boldsymbol{\psi}}|\boldsymbol{\psi}) = \frac{1}{\sqrt{\det(2\pi\boldsymbol{V})}} e^{-\frac{1}{2}(\hat{\boldsymbol{\psi}}-\boldsymbol{\psi})^T\boldsymbol{V}^{-1}(\hat{\boldsymbol{\psi}}-\boldsymbol{\psi})}. \quad (11)$$

Thus, the joint maximum likelihood (JML) estimator is

$$\begin{aligned}\hat{\boldsymbol{\theta}}_{JML} &= \arg\max_{\boldsymbol{\theta}} \ln p(\boldsymbol{r}, \hat{\boldsymbol{\psi}}|\boldsymbol{\theta}) \\ &= \arg\max_{\boldsymbol{\theta}} \sum_{m=1}^{M}\sum_{n=1}^{N} \frac{E_m \sigma_{mn}^2}{\sigma^2(\sigma^2 + K E_m \sigma_{mn}^2)} \left|\boldsymbol{r}_{mn}^H \boldsymbol{T}_{mn}(\boldsymbol{\theta})\right|^2 \\ &\quad - \frac{1}{2}(\hat{\boldsymbol{\psi}} - \boldsymbol{\psi})^T \boldsymbol{V}^{-1}(\hat{\boldsymbol{\psi}} - \boldsymbol{\psi}). \end{aligned} \tag{12}$$

3.2. Estimation With Known Ionospheric Parameter Distribution

Here we consider the scenario when the prior statistical information of the ionospheric parameters is available. Assume that the ionospheric parameter vector $\boldsymbol{\psi}$ is known to have a Gaussian prior distribution with mean $\boldsymbol{\mu}$ and covariance $\boldsymbol{\Sigma}$, such that

$$p(\boldsymbol{\psi}) = \frac{1}{\sqrt{\det(2\pi\boldsymbol{\Sigma})}} e^{-\frac{1}{2}(\boldsymbol{\psi}-\boldsymbol{\mu})^T \boldsymbol{\Sigma}^{-1}(\boldsymbol{\psi}-\boldsymbol{\mu})}. \tag{13}$$

In this case, the unknown parameter vector $\boldsymbol{\theta}$ to be estimated is composed of both random unknowns and deterministic unknowns, so the hybrid maximum likelihood and maximum a posteriori (ML/MAP) method [17] is employed to estimate $\boldsymbol{\theta}$. Considering that the observations $\boldsymbol{r}$ and $\hat{\boldsymbol{\psi}}$ are independent with each other, the joint probability density function (pdf) can be written as

$$p(\boldsymbol{r}, \hat{\boldsymbol{\psi}}, \boldsymbol{\psi}; \boldsymbol{\phi}) = p(\boldsymbol{r}, \hat{\boldsymbol{\psi}}|\boldsymbol{\psi}; \boldsymbol{\phi}) p(\boldsymbol{\psi}; \boldsymbol{\phi}) = p(\boldsymbol{r}|\boldsymbol{\theta})\, p(\hat{\boldsymbol{\psi}}|\boldsymbol{\psi}) p(\boldsymbol{\psi}).$$

Therefore, using (10), (11) and (13), the hybrid ML/MAP estimation can be obtained as

$$\begin{aligned}\hat{\boldsymbol{\theta}}_{HB} &= [\hat{\boldsymbol{\phi}}_{ML}^T, \hat{\boldsymbol{\psi}}_{MAP}^T]^T = \arg\max_{\boldsymbol{\theta}} \ln p\left(\boldsymbol{r}, \boldsymbol{\phi}, \hat{\boldsymbol{\psi}}; \boldsymbol{\phi}\right) \\ &= \arg\max_{\boldsymbol{\theta}} \sum_{m=1}^{M}\sum_{n=1}^{N} \frac{E_m \sigma_{mn}^2}{\sigma^2(\sigma^2 + K E_m \sigma_{mn}^2)} \left|\boldsymbol{r}_{mn}^H \boldsymbol{T}_{mn}(\boldsymbol{\theta})\right|^2 \\ &\quad - \frac{1}{2}(\hat{\boldsymbol{\psi}} - \boldsymbol{\psi})^T \boldsymbol{V}^{-1}(\hat{\boldsymbol{\psi}} - \boldsymbol{\psi}) - \frac{1}{2}(\boldsymbol{\psi} - \boldsymbol{\mu})^T \boldsymbol{\Sigma}^{-1}(\boldsymbol{\psi} - \boldsymbol{\mu}). \end{aligned} \tag{14}$$

4. JOINT ESTIMATION BOUNDS

This section derives performance bounds for the joint estimation with unknown or known prior ionospheric parameter distribution.

4.1. CRB for Unknown Ionospheric Parameter Distribution Case

When the prior distribution of the ionospheric parameters is unavailable, the mean square error (MSE) of the joint estimation of the deterministic unknown parameter vector is lower bounded by the Cramer-Rao bound (CRB) [18]. The CRB equals to the inverse of Fisher information matrix (FIM). From (9), it can be derived that the FIM for the joint estimation is

$$\boldsymbol{J}_F(\boldsymbol{\theta}) = \boldsymbol{J}_S(\boldsymbol{\theta}) + \boldsymbol{J}_I, \tag{15}$$

where $\boldsymbol{J}_I$ describes the contribution of the ionosonde,

$$\boldsymbol{J}_I = \mathbb{E}_{\hat{\boldsymbol{\psi}}|\boldsymbol{\psi}}\left\{\nabla_{\boldsymbol{\theta}} \ln p(\hat{\boldsymbol{\psi}}|\boldsymbol{\psi})[\nabla_{\boldsymbol{\theta}} \ln p(\hat{\boldsymbol{\psi}}|\boldsymbol{\psi})]^T\right\} = \begin{bmatrix} \mathbf{0} & \mathbf{0} \\ \mathbf{0} & \boldsymbol{V}^{-1} \end{bmatrix},$$

and $\boldsymbol{J}_S(\boldsymbol{\theta})$ describes the contribution of the radar received data,

$$\begin{aligned}\boldsymbol{J}_S(\boldsymbol{\theta}) &= \mathbb{E}_{\boldsymbol{r}|\boldsymbol{\theta}}\{[\nabla_{\boldsymbol{\theta}} \ln p(\boldsymbol{r}|\boldsymbol{\theta})][\nabla_{\boldsymbol{\theta}} \ln p(\boldsymbol{r}|\boldsymbol{\theta})]^T\} \\ &= \sum_{m=1}^{M}\sum_{n=1}^{N} \boldsymbol{J}_{mn}(\boldsymbol{\theta}), \end{aligned} \tag{16}$$

the ijth element of $\boldsymbol{J}_{mn}(\boldsymbol{\theta})$ is given by

$$\begin{aligned}[\boldsymbol{J}_{mn}(\boldsymbol{\theta})]_{ij} &= \frac{8\pi^2 E_m^2 \sigma_{mn}^4}{\sigma^2(\sigma^2 + K E_m \sigma_{mn}^2)} \\ &\quad \times \left(K \frac{\partial \boldsymbol{\varphi}_{mn}^H}{\partial \boldsymbol{\theta}_i} \frac{\partial \boldsymbol{\varphi}_{mn}}{\partial \boldsymbol{\theta}_j} - \mathbf{1}_{1\times K} \frac{\partial \boldsymbol{\varphi}_{mn}}{\partial \boldsymbol{\theta}_i} \mathbf{1}_{1\times K} \frac{\partial \boldsymbol{\varphi}_{mn}}{\partial \boldsymbol{\theta}_j}\right)\end{aligned}$$

in which $\mathbf{1}_{1\times K}$ denotes a $1 \times K$ vector of all ones, $\boldsymbol{\varphi}_{mn} = [\varphi_{mn}(\boldsymbol{\theta}, 1), \cdots, \varphi_{mn}(\boldsymbol{\theta}, K)]^T$ and

$$\frac{\partial \boldsymbol{\varphi}_{mn}}{\partial \boldsymbol{\theta}_i} = \left[\frac{\partial \varphi_{mn}(\boldsymbol{\theta}, 1)}{\partial \boldsymbol{\theta}_i}, \cdots, \frac{\partial \varphi_{mn}(\boldsymbol{\theta}, K)}{\partial \boldsymbol{\theta}_i}\right]^T, \tag{17}$$

$$\frac{\partial \varphi_{mn}(\boldsymbol{\theta}, k)}{\partial \boldsymbol{\theta}_i} = -\frac{f_m}{c}\left(\frac{\partial P_m^F(\boldsymbol{\theta}, k)}{\partial \boldsymbol{\theta}_i} + \frac{\partial P_n^B(\boldsymbol{\theta}, k)}{\partial \boldsymbol{\theta}_i}\right). \tag{18}$$

From (2) and (5), the first term inside the bracket of (18) is, for $i = 1, ..., 5$,

$$\frac{\partial P_m^F(\boldsymbol{\theta}, k)}{\partial \boldsymbol{\theta}_i} = \eta_{m,i}^F + \epsilon_m^F \frac{\partial \beta_m^F(\boldsymbol{\theta}, k)}{\partial \boldsymbol{\theta}_i}, \tag{19}$$

where $\eta_{m,1}^F = \eta_{m,2}^F = 0$, $\eta_{m,3}^F = b \ln \frac{1 + b \sin \beta_m^F(\boldsymbol{\theta}, k)}{1 - b \sin \beta_m^F(\boldsymbol{\theta}, k)}$,

$$\eta_{m,4}^F = \frac{2}{\sin \beta_m^F(\boldsymbol{\theta}, k)} - \eta_{m,3}^F,$$

$$\eta_{m,5}^F = -\frac{a}{f_o}\eta_{m,3}^F - \frac{2ab^2 \sin \beta_m^F(\boldsymbol{\theta}, k)}{f_o(1 - b^2 \sin^2 \beta_m^F(\boldsymbol{\theta}, k))},$$

$$\epsilon_m^F = -\frac{2y_b \cos \beta_m^F(\boldsymbol{\theta}, k)}{\sin^2 \beta_m^F(\boldsymbol{\theta}, k)} + \frac{2ab^2 \cos \beta_m^F(\boldsymbol{\theta}, k)}{1 - b^2 \sin^2 \beta_m^F(\boldsymbol{\theta}, k)}.$$

The last term on the right hand side of (19) can be computed by taking the derivative with respect to $\boldsymbol{\theta}_i$ on both sides of (6), which is

$$\frac{\partial \beta_m^F(\boldsymbol{\theta}, k)}{\partial \boldsymbol{\theta}_i} = \frac{\eta_{m,i}^F - \kappa_{m,i}^F}{\nu_m^F - \epsilon_m^F} \tag{20}$$

where $\nu_m^F = (x + vkT_r - x_m^T)\tan \beta_m^F(\boldsymbol{\theta}, k) \sec \beta_m^F(\boldsymbol{\theta}, k)$,

$$\kappa_{m,i}^F = \begin{cases} \sec \beta_m^F(\boldsymbol{\theta}, k) & i = 1 \\ kT_r \sec \beta_m^F(\boldsymbol{\theta}, k) & i = 2 \\ 0 & i = 3, 4, 5 \end{cases}. \tag{21}$$

Similarly, we can derive $\partial P_m^B(\boldsymbol{\theta}, k)/\partial \boldsymbol{\theta}_i$. Substituting the above expressions and (16) into (15), we can obtain the FIM $\boldsymbol{J}_F(\boldsymbol{\theta})$. The CRB of $\boldsymbol{\theta}_i$, the ith element of $\boldsymbol{\theta}$, can be calculated as

$$\text{CRB}(\boldsymbol{\theta}_i) = [\boldsymbol{J}_F^{-1}(\boldsymbol{\theta})]_{ii}, i = 1, \cdots, 5. \tag{22}$$

4.2. HCRB for Known Ionospheric Parameter Distribution Case

For the case where the prior distribution of the ionospheric parameters is available, the MSE of the joint estimation of the partially random and partially deterministic unknown parameter vector is lower bounded by the hybrid CRB (HCRB), which is the inverse of the hybrid information matrix [18]

$$\boldsymbol{J}_{HB} = \boldsymbol{J}_M + \boldsymbol{J}_P, \tag{23}$$

where $\boldsymbol{J}_P$ is determined by the ionospheric parameter prior distribution,

$$\boldsymbol{J}_P = \left[\begin{array}{cc} \mathbf{0} & \mathbf{0} \\ \mathbf{0} & \boldsymbol{\Sigma}^{-1} \end{array} \right], \tag{24}$$

and $\boldsymbol{J}_M$ describes the contribution of the measured data,

$$\boldsymbol{J}_M = \mathbb{E}_{\boldsymbol{\psi}} \left\{ \boldsymbol{J}_F \left(\boldsymbol{\theta} \right) \right\} = \mathbb{E}_{\boldsymbol{\psi}} \left\{ \boldsymbol{J}_S \left(\boldsymbol{\theta} \right) \right\} + \boldsymbol{J}_I, \tag{25}$$

in which $\boldsymbol{J}_S(\boldsymbol{\theta})$ and $\boldsymbol{J}_I$ are defined in (15). Therefore, taking the inverse of $\boldsymbol{J}_{HB}$, the HCRB associated with the estimate of $\boldsymbol{\theta}_i$ can be obtained as

$$\text{HCRB}_i = \left[\boldsymbol{J}_{HB}^{-1} \right]_{ii}, i = 1, \cdots, 5. \tag{26}$$

5. NUMERICAL RESULTS

Consider a MIMO-OTH radar system with $M = 3$ transmitters and $N = 3$ receivers located at $(0,0), (1,0), (2,0) km$ and $(3,0), (4,0), (5,0) km$, respectively. The carrier frequencies of the transmitted signals are set to 5, 10 and $15 MHz$. Assume $T_r = 0.02s$, $K = 500$ and $E_m = E = 1$. The variances of target reflection coefficients are $\sigma_{mn}^2 = \sigma_\alpha^2 = 1$. The signal to noise ratio (SNR) is defined as SNR$= E\sigma_\alpha^2/\sigma^2$. Without loss of generality and to reduce simulation load, assume that y_b, f_o, and v in $\boldsymbol{\theta}$ are known to be $110km$, $4MHz$, and $20m/s$ respectively, so that only the ionospheric height y_o and the target position x need to be estimated.

1) Examples for Unknown Ionospheric Parameter Distribution: Assume that the true values of the unknown parameters are $y_o = 150km$ and $x = 1500km$. In Figs.1(a) and 1(b), the MSEs of the JML estimates of y_o and x are plotted versus SNR, respectively. In both figures, we see that the curves for $V = 10$ are higher than the ones for $V = 1$, which implies that smaller V leads to better MSE performance, as expected. It is observed that the MSEs of the JML estimation are close to the CRBs, which verifies the correctness of the CRB derivation in Section 4.1. For comparison, in the same figures we also plot the MSEs obtained using the traditional estimation method (TEM), where the estimate $\hat{y}_o$ of y_o is calculated by the ionosonde solely and then passed to the OTH radar which takes this estimated value as if it were the true value to further estimate x. In this case the variance of the TEM for y_o is exactly equal to the error variance V (see the curves marked with squares in Fig.1(a)). In Fig.1(b), we find that the MSE of JML is smaller than that of TEM for all SNRs, which shows that the joint estimation is always superior to the non-joint estimation in the statistical sense. It is also seen that when the SNR is small, the MSE of TEM is close to the MSE of JML, but when the SNR exceeds a threshold (see arrows in the figures) the MSE of TEM is approximately constant and the gap between the MSE of TEM and MSE/CRB of JML increases with the increasing SNR. Intuitively, in the traditional OTH radars, the estimation error of $\hat{y}_o$ is totally determined by the ionosonde, which cannot be improved even if the SNR of the

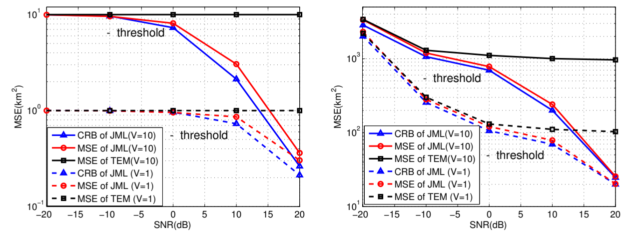

(a) Performance of y_o (b) Performance of x

Fig. 1. MSE of JML and TEM.

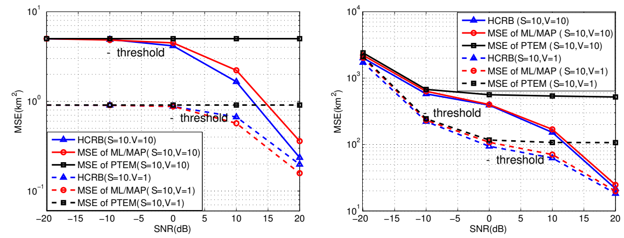

(a) Performance of y_o (b) Performance of x

Fig. 2. MSE of PTEM and ML/MAP.

radar received signals is large (see Fig.1(a)), and thus limits the estimation accuracy of x. The JML estimation makes use of the received signals for the estimation of y_o and x, which enables the improvement of the estimation accuracy for both y_o and x when the SNR becomes larger.

2) Examples for Known Ionospheric Parameter Distribution: Assume the prior distribution of the ionospheric parameter y_o is known to be Gaussian with mean $\mu = 150km$ and variance $\Sigma = 10km^2$, such that the MIMO-OTH radar can use this prior distribution for parameter estimation. The MSEs of the estimates obtained from the proposed joint estimation (ML/MAP) are plotted versus SNR in Figs.2(a) and 2(b). The MSE curves obtained using the traditional methods (PTEM) are also provided for comparison. It is seen that the MSEs of ML/MAP estimation are close to the HCRBs, which verifies the correctness of the HCRB derivation in Section 4.2. Again, the solid curve for $V = 10$ it above the ones for $V = 1$, which indicates that smaller V leads to better MSE performance. It is observed that the proposed method always performs better than the tradition method. The performance gain is insignificant when the SNR is small, whereas as the SNR increases and exceeds a threshold the performance gain of the joint estimation is dramatic.

6. CONCLUSION

Joint estimation of the ionospheric and target parameters was studied for MIMO-OTH radar. We presented JML and ML/MAP joint estimation for two scenarios where prior distribution of ionospheric parameters is either known or unknown, respectively. The CRB and HCRB associated with known and unknown prior distribution cases were developed. The simulation results showed that the proposed joint methods can improve the estimation accuracy of the target parameters via more effective usage of the radar received signals.

7. REFERENCES

[1] J. Headrick and J. Thomason, “Applications of high-frequency radar,” *Radio Science*, vol. 33, no. 4, pp. 1045–1054, 1998.

[2] H. Godrich, A. P. Petropulu, and H. V. Poor, “Power allocation strategies for target localization in distributed multiple-radar architectures,” *Signal Processing, IEEE Transactions on*, vol. 59, no. 7, pp. 3226–3240, 2011.

[3] X. Song, P. Willett, S. Zhou, and P. B. Luh, “The mimo radar and jammer games,” *Signal Processing, IEEE Transactions on*, vol. 60, no. 2, pp. 687–699, 2012.

[4] J. Li and P. Stoica, *MIMO radar signal processing*. Wiley. com, 2008.

[5] P. Wang, H. Li, and B. Himed, “Moving target detection using distributed mimo radar in clutter with nonhomogeneous power,” *Signal Processing, IEEE Transactions on*, vol. 59, no. 10, pp. 4809–4820, 2011.

[6] E. Fishler, A. Haimovich, R. Blum, D. Chizhik, L. Cimini, and R. Valenzuela, “MIMO radar: an idea whose time has come,” in *Radar Conference, 2004. Proceedings of the IEEE*, pp. 71–78, IEEE, 2004.

[7] Q. He, R. S. Blum, and A. M. Haimovich, “Noncoherent MIMO radar for location and velocity estimation: More antennas means better performance,” *Signal Processing, IEEE Transactions on*, vol. 58, no. 7, pp. 3661–3680, 2010.

[8] Y. D. Zhang, J. J. Zhang, M. G. Amin, and B. Himed, “Instantaneous altitude estimation of maneuvering target in over-the-horizon radar exploiting multipath Doppler signatures,” *EURASIP Journal on Advances in Signal Processing*, vol. 2013, no. 1, p. 100, 2013.

[9] G. J. Frazer, Y. I. Abramovich, and B. A. Johnson, “Multiple-input multiple-output over-thehorizon radar: experimental results,” *IET Radar, Sonar Navigation*, vol. 3, pp. 290–303, Aug. 2009.

[10] K. Davies, *Ionospheric Radio*. London, United Kingdom: Institution of Engineering and Technology, 1990.

[11] N. N. Rao, “Analysis of discrete oblique ionogram traces in sweep-frequency sky-wave high resolution backscatter,” *Radio Science*, vol. 10, p. 149C153, Feb. 1975.

[12] T. Landeau, F. Gauthier, and N. Ruelle, “Further improvements to the inversion of elevation-scan backscatter sounding data,” *Journal of Atmospheric and Terrestrial Physics*, vol. 59, pp. 125–138, Jan. 1997.

[13] S. V. Fridman, L. Nickisch, and M. Hausman, “Inversion of backscatter ionograms and TEC data for over-the-horizon radar,” *Radio Science*, vol. 47, no. 2, 2012.

[14] P. Dyson and J. Bennett, “A model of the vertical distribution of the electron concentration in the ionosphere and its application to oblique propagation studies,” *Journal of Atmospheric and Terrestrial Physics*, vol. 50, p. 251C262, Mar. 1988.

[15] R.J.Norman, “Backscatter Ionogram Inversion,” *Radio Science*, vol. 41, pp. 368–374, 2003.

[16] J. R. Hill, “Exact ray paths in a multisegment quasi-parabolic ionosphere,” *Radio Science*, vol. 14, pp. 855–861, Sep.-Oct. 1979.

[17] Y. Rockah and P. M. Schultheiss, “Array Shape Calibration Using Sources in Unknown Locations-part I: Near-Field Sources,” *IEEE Transactions Acoust., Speech, Signal Process*, vol. 35, pp. 286–299, Mar. 1987.

[18] H. L. V. Trees and K. L. Bell, *Bayesian Bounds for Parameter Estimation and Nonlinear Filtering/Tracking*. New York: Wiley-IEEE Press, 2007.